responses. By experimentally probing this space, we are able to gain quantitative insight into the architecture, dynamics and design constraints of biological systems. □

Methods

Bacterial strains and plasmids

The *gfp* gene under the control of the wild-type *lac* promoter, obtained from plasmid pGFPmut3.1 (Clontech), was inserted into the chromosome of *E. coli* MG1655 at the lambda insertion site using the λ-InCH technique[29] to produce the strain MUK21. The *gat* promoter was amplified from the *E. coli* MG1655 chromosome by polymerase chain reaction using primers flanking the 2,175,231–2,175,531 chromosomal region. The *HcRed* gene was obtained from pHcRed1–C1 (Clontech) and was placed under the control of the *gat* promoter into a plasmid with a ColE1 replication origin, which was transformed into MUK21 cells to obtain the strain ERT113. All measurements of wild-type network response were conducted in this strain. Two additional strains with *lac* operon repression factors at lower levels than in the wild-type were constructed by transforming MUK21 cells with multicopy plasmids, each incorporating a single copy of the *lac* promoter. The strain MUK21-pSC101* contains plasmids with a pSC101* replication origin (average copy number 4), and the strain MUK21-p15A contains plasmids with a p15A replication origin (average copy number 25)[30].

Growth conditions and media

Cells were grown at 37 °C in M9 minimal medium with succinate as the main carbon source, supplemented with varying amounts of glucose and TMG. Master cultures with cells induced for *lac* expression were prepared by overnight growth in 1 mM TMG, and master cultures with uninduced cells by overnight growth in the absence of TMG. During each experimental run, cells were transferred from these master cultures into media containing specified amounts of glucose and TMG. They were subsequently grown for 20 additional hours before they were harvested for measurement. The transfer volume was calculated to produce extremely low final cell densities (OD_{600}~0.001), thereby preventing the depletion of glucose and TMG from the medium. Cells were concentrated by filtration and centrifugation, and the resulting pellet was resuspended in 2.5 μl of the growth medium to prepare a microscope slide.

Data acquisition

Green and red fluorescence values of single cells were measured using a Nikon TE2000 microscope with automated stage and focus. For each experiment, images of about 1,000 cells on each slide were collected using a cooled back-thinned CCD camera (Micromax, Roper Scientific). These images were analysed using Metamorph (Universal Imaging) to obtain the average fluorescence of each cell above the fluorescence background.

Data analysis

For each glucose concentration, the fraction of cells in the induced state was determined as a function of TMG concentration, and the switching thresholds (defined as the TMG concentrations at which less than 5% of the cells are in their initial states) were obtained by interpolation. We estimated the green fluorescence values of the induced (high) and uninduced (low) subpopulations at each switching threshold by averaging over two neighbouring TMG concentrations. At each threshold, the high fluorescence was a linear function of the low fluorescence, with a small positive intercept comparable to the autofluorescence of *E. coli* MG1655 cells. We interpreted this intercept as the autofluorescence of the ERT113 strain. The repression factors for the MUK21-pSC101* and MUK21-p15A strains were estimated by taking the ratio of fully induced to uninduced fluorescence levels, assuming that these strains had the same autofluorescence background as ERT113.

Received 8 November; accepted 16 December 2003; doi:10.1038/nature02298.

1. Ferrell, J. E. Jr & Machleder, E. M. The biochemical basis of an all-or-none cell fate switch in *Xenopus* oocytes. *Science* **280,** 895–898 (1998).
2. Pomerening, J. R., Sontag, E. D. & Ferrell, J. E. Jr Building a cell cycle oscillator: hysteresis and bistability in the activation of Cdc2. *Nature Cell Biol.* **5,** 346–351 (2003).
3. Sha, W. *et al.* Hysteresis drives cell-cycle transitions in *Xenopus laevis* egg extracts. *Proc. Natl Acad. Sci. USA* **100,** 975–980 (2003).
4. Hernday, A., Braaten, B. A. & Low, D. The mechanism by which DNA adenine methylase and PapI activate the pap epigenetic switch. *Mol. Cell* **12,** 947–957 (2003).
5. Blauwkamp, T. A. & Ninfa, A. J. Physiological role of the GlnK signal transduction protein of *Escherichia coli*: survival of nitrogen starvation. *Mol. Microbiol.* **46,** 203–214 (2002).
6. Siegele, D. A. & Hu, J. C. Gene expression from plasmids containing the araBAD promoter at subsaturating inducer concentrations represents mixed populations. *Proc. Natl Acad. Sci. USA* **94,** 8168–8172 (1997).
7. Gardner, T. S., Cantor, C. R. & Collins, J. J. Construction of a genetic toggle switch in *Escherichia coli*. *Nature* **403,** 339–342 (2000).
8. Isaacs, F. J., Hasty, J., Cantor, C. R. & Collins, J. J. Prediction and measurement of an augoregulatory genetic module. *Proc. Natl Acad. Sci. USA* **100,** 7714–7719 (2003).
9. Becskei, A., Seraphin, B. & Serrano, L. Positive feedback in eukaryotic gene networks: cell differentiation by graded to binary response conversion. *EMBO J.* **20,** 2528–2535 (2001).
10. Ferrell, J. E. Jr Self-perpetuating states in signal transduction: positive feedback, double-negative feedback and bistability. *Curr. Opin. Cell Biol.* **14,** 140–148 (2002).
11. Ma, S.-K. *Modern Theory of Critical Phenomena* (Perseus Books, Reading, Massachusetts, 1976).
12. Strogatz, S. H. *Nonlinear Dynamics and Chaos* (Perseus Books, Reading, Massachusetts, 1994).
13. Müller-Hill, B. *The Lac Operon: A Short History of a Genetic Paradigm* (Walter de Gruyter, Berlin, 1996).
14. Louis, M. & Becskei, A. Binary and graded responses in gene networks. *Science STKE* [online], 30 July 2002 (doi:10.1126/stke.2002.143.pe33).
15. Biggar, S. R. & Crabtree, G. R. Cell signaling can direct either binary or graded transcriptional responses. *EMBO J.* **20,** 3167–3176 (2001).
16. Novick, A. & Weiner, M. Enzyme induction as an all-or-none phenomenon. *Proc. Natl Acad. Sci. USA.* **43,** 553–566 (1957).
17. Cohn, M. & Horibata, K. Inhibition by glucose of the induced synthesis of the β-galactoside-enzyme system of *Escherichia coli*: Analysis of maintenance. *J. Bacteriol.* **78,** 601–612 (1959).
18. Stulke, J. & Hillen, W. Carbon catabolite repression in bacteria. *Curr. Opin. Microbiol.* **2,** 195–201 (1999).
19. Setty, Y., Mayo, A. E., Surette, M. G. & Alon, U. Detailed map of a *cis*-regulatory input function. *Proc. Natl Acad. Sci. USA* **100,** 7702–7707 (2003).
20. Griffith, J. S. Mathematics of cellular control processes II: Positive feedback to one gene. *J. Theor. Biol.* **20,** 209–216 (1968).
21. Tyson, J. J. & Othmer, H. G. The dynamics of feedback control circuits in biochemical pathways. *Prog. Theor. Biol.* **5,** 1–62 (1978).
22. Nobelmann, B. & Lengeler, J. W. Molecular analysis of the *gat* genes from *Escherichia coli* and of their roles in galactitiol transport and metabolism. *J. Bacteriol.* **178,** 6790–6795 (1996).
23. Oehler, S., Eismann, E. R., Kramer, H. & Müller-Hill, B. The three operators of the *lac* operon cooperate in repression. *EMBO J.* **9,** 973–979 (1990).
24. Chung, J. D. & Stephanopoulos, G. On physiological multiplicity and population heterogeneity of biological systems. *Chem. Eng. Sci.* **51,** 1509–1521 (1996).
25. Kepler, T. B. & Elston, T. C. Stochasticity in transcriptional regulation: origins, consequences, and mathematical representations. *Biophys. J.* **81,** 3116–3136 (2001).
26. Thattai, M. & Shraiman, B. I. Metabolic switching in the sugar phosphotransferase system of *Escherichia coli*. *Biophys. J.* **85,** 744–754 (2003).
27. Atkinson, M. R., Savageau, M. A., Myers, J. T. & Ninfa, A. J. Development of genetic toggle circuitry exhibiting toggle switch or oscillatory behavior in *Escherichia coli*. *Cell* **113,** 597–607 (2003).
28. Smolen, P., Baxter, D. A. & Byrne, J. H. Frequency selectivity, multistability, and oscillations emerge from models of genetic regulatory systems. *Am. J. Physiol.* **43,** C531 (1998).
29. Boyd, D., Weiss, D. S., Chen, J. C. & Beckwith, J. Towards single-copy gene expression systems making gene cloning physiologically relevant: lambda InCh, a simple *Escherichia coli* plasmid-chromosome shuttle system. *J. Bacteriol.* **182,** 842–847 (2000).
30. Lutz, R. & Bujard, H. Independent and tight regulation of transcriptional units in *Escherichia coli* via the LacR/O, the TetR/O and AraC/I1-I2 regulatory elements. *Nucleic Acids Res.* **25,** 1203–1210 (1997).

Supplementary Information accompanies the paper on **www.nature.com/nature**.

Acknowledgements We thank G. Jacobson and H. Kornberg, J. Paulsson, M. Savageau and A. Sengupta for discussions and suggestions; H. Bujard and R. Lutz for supplying the pZ vector system; and D. Boyd for help with the λ-InCh technique. We thank D. Raut for his assistance with the initial lactose measurements and the construction of plasmids and strains. We also thank A. Becskei and J. Pedraza for critically reviewing the manuscript. This work was supported by NIH and DARPA grants, and an NSF-CAREER grant.

Competing interests statement The authors declare that they have no competing financial interests.

Correspondence and requests for materials should be addressed to A.v.O. (avano@mit.edu).

Unique astrocyte ribbon in adult human brain contains neural stem cells but lacks chain migration

Nader Sanai[1,2], Anthony D. Tramontin[1,2], Alfredo Quiñones-Hinojosa[1], Nicholas M. Barbaro[1], Nalin Gupta[1], Sandeep Kunwar[1], Michael T. Lawton[1], Michael W. McDermott[1], Andrew T. Parsa[1], José Manuel-García Verdugo[3], Mitchel S. Berger[1] & Arturo Alvarez-Buylla[1,2]

[1]*Department of Neurological Surgery and Brain Tumor Research Center, and* [2]*Developmental Stem Cell Biology Program, University of California San Francisco, San Francisco, California 94143, USA*
[3]*Instituto Cavanilles, University of Valencia, 46100, Spain*

The subventricular zone (SVZ) is a principal source of adult neural stem cells in the rodent brain, generating thousands of olfactory bulb neurons every day[1]. If the adult human brain contains a comparable germinal region, this could have considerable implications for future neuroregenerative therapy. Stem cells have been isolated from the human brain[2–7], but the identity, organization and function of adult neural stem cells in the

human SVZ are unknown. Here we describe a ribbon of SVZ astrocytes lining the lateral ventricles of the adult human brain that proliferate *in vivo* and behave as multipotent progenitor cells *in vitro*. This astrocytic ribbon has not been observed in other vertebrates studied. Unexpectedly, we find no evidence of chains of migrating neuroblasts in the SVZ or in the pathway to the olfactory bulb. Our work identifies SVZ astrocytes as neural stem cells in a niche of unique organization in the adult human brain.

Young neurons born in the rodent and primate SVZ migrate in chains through the rostral migratory stream (RMS) to replace interneurons of the olfactory bulb[8–10]. Data from rodents indicate that SVZ neural stem cells are astrocytes[11–14]. In the presence of exogenous mitogens, SVZ-derived neural stem cells self-renew and can differentiate into astrocytes, oligodendrocytes and neurons *in vitro*[15–17]. Explants of intraoperative and postmortem adult human brain also contain progenitors that can give rise to new neurons and glia[2,4,6,7,18,19], but the organization and function of the human germinal zones that contain these progenitors remain poorly understood.

We collected adult human SVZ specimens from 65 neurosurgical resections and 45 autopsied brains (Fig. 1a; specimens are listed in Supplementary Tables 1 and 2). With a starting concentration of 50,000 cells per ml (refs 15, 17), intraoperative samples from the anterior horn, body, atrium, occipital horn and temporal horn of the lateral ventricular walls generated on average 62.57 ± 7.46 (mean ± s.d.) neurospheres per ml in the presence of epidermal growth factor (EGF) and fibroblast growth factor (FGF). On average, 33.11 ± 3.81 secondary neurospheres were generated from 100 primary neurospheres.

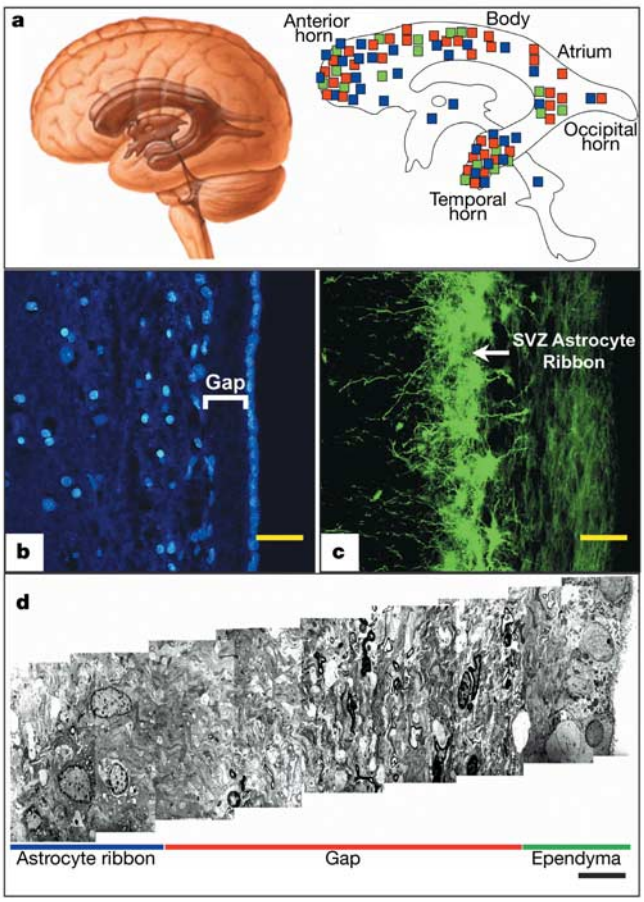

Figure 1 Dense ribbon of SVZ astrocytes in the adult human brain. **a**, SVZ specimen locations along lateral wall of the human ventricles. Intraoperative tissue was used for histology (red) and culture (green) experiments. Autopsied tissue (blue) was used only for histology. **b**, Coronal section (6 μm) stained with the nuclear marker DAPI reveals a region of high cellularity that is separated from the ependyma by a gap. **c**, Vibratome section showing GFAP expression of SVZ astrocyte ribbon and GFAP-positive fibre bundles filling the subependymal gap. **d**, Panoramic electron micrograph of a postmortem adult human SVZ, showing the ependymal lining, gap region and astrocyte ribbon. Scale bars, 40 μm (**b**, **c**); 10 μm (**d**).

Human SVZ neurospheres differentiated into glia fibrillary acidic protein (GFAP)-positive astrocytes, O4-positive oligodendrocytes and TuJ1-positive neurons. Primary neurospheres ($n = 35$ independent samples) yielded 6.5 ± 3.4% neurons, 5.8 ± 1.5% oligodendrocytes and 87.8 ± 3.1% astrocytes. In parallel, specimens that excluded the SVZ, including parietal cortex ($n = 8$), temporal cortex ($n = 10$), striatum ($n = 14$), medial (septal) wall of the lateral ventricle ($n = 3$), third ventricle ($n = 2$) and fourth ventricle ($n = 1$), did not generate neurospheres. Our results indicate that EGF- and FGF-responsive precursors exist not only in the temporal lobe[4,7], but in samples from different regions of the lateral walls of the human lateral ventricles.

Sections of adult human SVZ specimens ($n = 68$) showed a band of cells separated from the ependyma (Fig. 1b). Most cells in this band were astrocytes, showing stellate morphology and expressing GFAP (Fig. 1c) and vimentin (data not shown). This astrocyte ribbon was present in intraoperative and autopsied specimens from the lateral ventricular walls of male and female individuals aged 19–68 yr. It was not observed, however, along the third or fourth ventricles ($n = 3$), nor was it present in samples of the medial (septal) wall of the lateral ventricles ($n = 6$). This astroglia band has not been described in the SVZ of primates[8,10], rodents[20], dogs[21], cows[22] or sheep (unpublished observations), and represents a departure from classical SVZ cytoarchitecture[20].

Under the electron microscope, cells in the band had ultrastructural characteristics of astrocytes (Figs 1d and 2a). Astrocytes in the SVZ ribbon were separated from the ependyma by a gap filled with GFAP-positive processes (Supplementary Fig. 1). These processes contained intermediate filaments and gap junctions (Fig. 2b), confirming their astrocytic origin. No chains of migratory neuroblasts were seen in the ribbon or gap, although occasionally single, elongated, TuJ1-positive cells were observed (Supplementary Fig 3b). A few astrocyte somata were also found in the gap region (Fig. 2c). Notably, some of these astrocytes had a process extending into ependyma, towards the ventricular lumen (Fig. 2d).

Some cells in the astrocyte ribbon coexpressed GFAP and the cell-division marker Ki-67, suggesting that a subpopulation of them were mitotically active *in vivo* (Fig. 2e). To confirm this observation, organotypic slices of human SVZ ($n = 3$) were incubated in medium containing 5-bromodeoxyuridine (BrdU). After 36 h, an antibody against BrdU was found to colocalize with GFAP-positive cells in the SVZ ribbon (Supplementary Fig. 2). In a study of individuals treated with BrdU, proliferative SVZ cells were found in the same position[23]. Taken together, these findings indicate that cells in this band of SVZ astrocytes divide *in vivo*. From Ki-67 labelling ($n = 10$ total specimens), we estimated that 0.77 ± 0.29% of astrocytes in the SVZ ribbon were in division. Cultures of microdissected adult human SVZ yielded monolayers of astrocytes. Notably, in comparison to cortical astrocyte cultures, SVZ astrocytes grew at a considerably higher rate (Fig. 3a).

We next examined whether adult human SVZ astrocytes could produce multipotent, self-renewing neurospheres. Cultures of SVZ astrocytes ($n = 25$ specimens) were dissociated and incubated in serum-free medium containing EGF and basic FGF (bFGF). Seeding at an initial concentration of 50,000 astrocytes per ml, we generated 109.29 ± 8.67 neurospheres per ml.

We then tested whether single human SVZ astrocytes could produce multipotent, self-renewing neurospheres. SVZ astrocyte cultures were established from the lateral walls of the anterior horn ($n = 3$), body ($n = 2$) and temporal horn ($n = 3$). Cells were

incubated for 3 d with an adenovirus carrying the gene for green fluorescent protein (GFP) controlled by the GFAP promoter (GFAPp)[11]. Single green astrocytes were individually micropipetted into separate wells of conditioned neurosphere medium. Of 121 anterior horn SVZ astrocytes plated, 5 (4.1%) generated clonal neurospheres. Similarly, of 113 ventricle body SVZ astrocytes and 137 temporal horn SVZ astrocytes, 4 (3.5%) and 4 (2.9%) clonal neurospheres were produced, respectively. Dissociation of the neurospheres derived from single astrocytes resulted in the production of secondary neurospheres. On the differentiation of primary and secondary neurospheres, we identified astrocytes, oligodendrocytes and neurons in each colony (Fig. 3b). Single cortical astrocytes (139 tested) and single astrocytes derived from tissue adjacent to the SVZ (201 tested) did not generate neurospheres. These experiments indicate that human SVZ neural stem cells correspond to astrocytes.

The high concentrations of exogenous mitogens required for neurosphere formation may amplify the true capabilities of a cell. We therefore tested whether primary SVZ astrocytes generate neurons without EGF, bFGF or neurosphere formation. In the absence of exogenous EGF and FGF, a substrate of astrocytes can support neurogenesis for adult neural stem cells[24,25]. Cultured SVZ astrocytes from the anterior horn ($n = 8$ specimens) were incubated with the GFAPp–GFP adenovirus and the nuclear marker 4′,6-diamidino-2-phenylindole dihydrochloride (DAPI). Single green astrocytes were placed onto human cortical astrocyte monolayers in serum-free medium (Fig. 3c, inset). At 5–14 d *in vitro*, 5 out of 64 (7.8%) SVZ astrocytes generated colonies with bipolar and/or multipolar cells expressing DAPI and TuJ1 (Fig. 3c). By contrast, single cortical astrocytes ($n = 80$) placed under identical conditions yielded only astrocytes. These observations provide direct evidence that single adult human SVZ astrocytes, in the absence of exogenous growth factors, are capable of neurogenesis.

New neurons born in the SVZ migrate in chains along the RMS. This migration is well documented in many adult mammalian species[26,27], including primates[8,10], but not in humans. The large pool of SVZ neuronal progenitors that we describe suggested that a similar migration might occur in adult humans. However, we found no evidence of neuronal chain migration in the SVZ. Serial coronal and sagittal sections ($n = 9$ total specimens; Fig. 4a) did reveal a structure beginning at the ventral floor of the anterior horn and coursing ventro-rostrally to the olfactory trigone—the origin of the human olfactory peduncle (Fig. 4b). This SVZ–olfactory trigone connection contained displaced ependymal cavities (Fig. 4b, inset), hallmarks of descent from an embryonic olfactory ventricle that precedes the adult RMS. Nissl staining and double labelling for TuJ1 and polysialylated neural cell adhesion molecule (PSA-NCAM)[8,10] did not show evidence of chains of young migratory neurons in this region. Cells in this human SVZ–olfactory trigone connection were rich in GFAP (Fig. 4c), suggesting that this region contains many astrocytes.

Regardless of their route out of the SVZ, chains of newly generated neurons, if present, must traverse the human olfactory peduncle to reach the bulbs. Under the light microscope, the olfactory peduncle was composed of a network of myelinated axons, corpus amylaceum[28], astrocytes and GFAP-positive processes (Fig. 4d, e, and Supplementary Fig. 4c), but devoid of TuJ1-positive or PSA-NCAM-positive chain-migrating neurons (Fig. 4f and Supplementary Fig. 4b). Rarely, an elongated cell expressing TuJ1 was observed, but these cells were not organized into chains. Expression of TuJ1 in this and other human brain regions (Supplementary Fig. 3a) served as a positive control, indicating that any lack of labelling was not due to antibody incompatibility with human material. We confirmed these results by electron microscopy of serial semithin sections of intraoperative and postmortem olfactory peduncle ($n = 12$ total specimens; Fig. 4d and Supplementary Fig. 4a). Again, we found no evidence of chains of migrating neurons in the olfactory peduncle or a structure similar

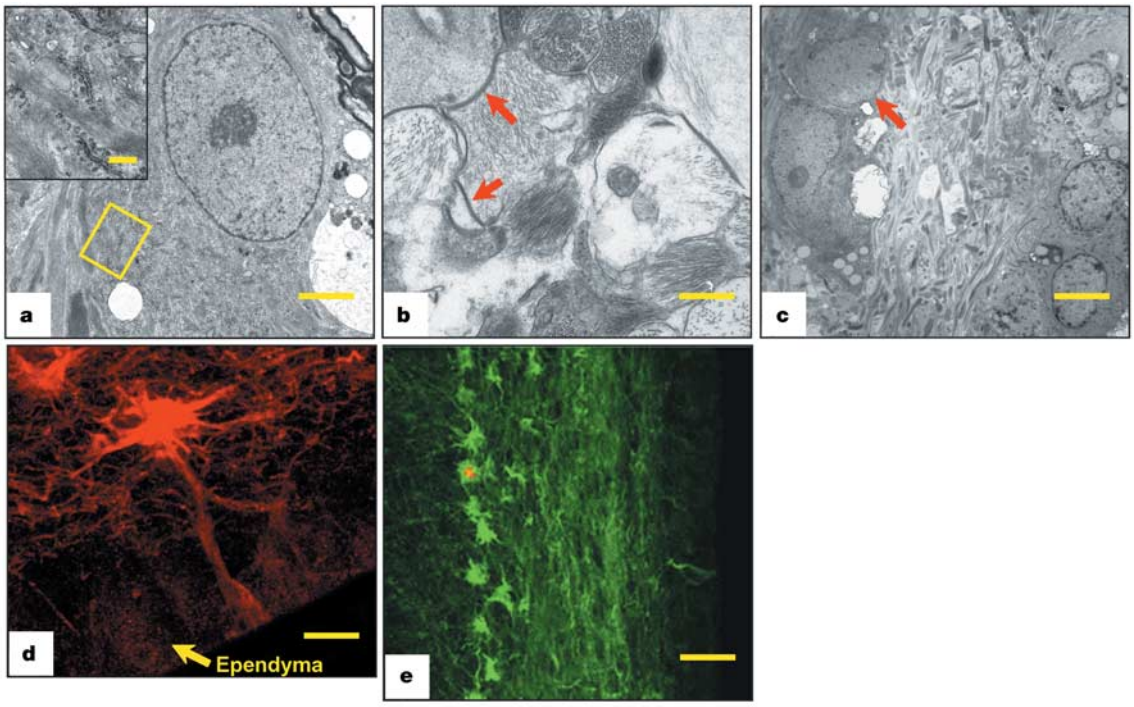

Figure 2 Characteristics of adult human SVZ astrocytes. **a**, Electron micrograph of the SVZ ribbon identifies an astrocyte nucleus with a cell body containing copious intermediate filaments (inset) and rough endoplasmic reticulum. **b**, SVZ gap region contains many astrocytic processes and a network of gap junctions. **c**, Nuclei (red arrows) of two displaced astrocytes in the gap region. Notice how these cells are surrounded by other astrocytic processes in the gap. Nearby ependymal lining is seen on the right. **d**, Displaced SVZ astrocyte soma extends a process towards the lateral ventricle. **e**, Ki-67 labelling (red) colocalizing to a proliferating GFAP-positive astrocyte (green) in the SVZ ribbon. Scale bars, 1.5 μm (**a**); 0.1 μm (**a**, inset); 1 μm (**b**); 3 μm (**c**); 7 μm (**d**); 40 μm (**e**).

to the RMS of other mammals. These findings raise the unexpected possibility that migration from the SVZ to the olfactory bulb does not take place in adult humans or, if it does, precursors migrate as individual cells.

We have described a subventricular organization in the adult human brain that differs considerably from that of other vertebrates that have been studied. This germinal region contains cells with astrocytic characteristics that can function as neural stem cells and features a previously uncharacterized periventricular astrocyte ribbon. Although the precise location of the stem cells cannot be established, we know that astrocytes from this region are clonal precursors of self-renewing, multipotent neurospheres and can give rise to neurons in the absence of exogenous growth factors. Considering the size of the human lateral ventricular system, our work suggests that a substantial number of neural stem cells exist in the adult brain throughout life.

Despite such robust germinal capacity, there is no evidence of cells migrating in chains along the SVZ or olfactory peduncle to the bulb. This may be explained by the long distance that separates the olfactory bulbs from the cerebrum in humans and/or our relatively micro-osmatic capabilities. Our findings raise the question of the fate of cells born in the human SVZ. The identification of a large, anatomically discrete population of proliferating, multipotent human astrocytes may also lead to a better understanding of the role that human neural stem cells have in tumorigenesis, demyelination and neurodegeneration. This work highlights the importance of studying stem cells in the human brain. □

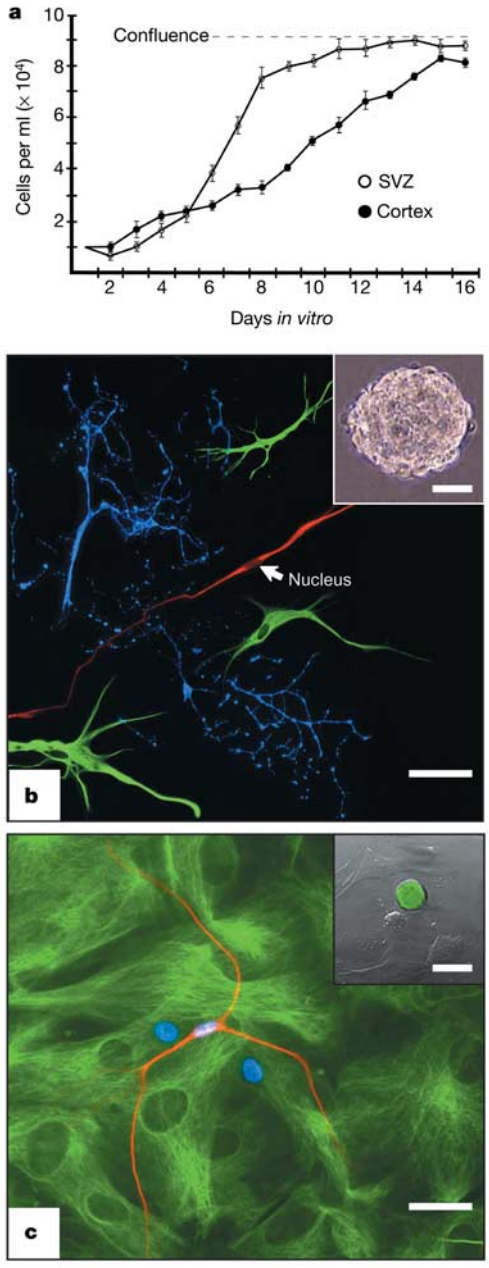

Figure 3 Human SVZ astrocytes as neural progenitors. **a**, Proliferation rates for SVZ and cortical astrocytes were significantly different ($P < 0.05$). **b**, Single SVZ astrocytes generated clonal neurospheres (inset) that differentiate into TuJ1-positive neurons (red), GFAP-positive astrocytes (green) and O4-positive oligodendrocytes (blue). **c**, Single SVZ astrocytes transfected with a GFAPp–GFP adenovirus fluoresced green and were placed on a cortical astrocyte monolayer; inset shows superimposed differential interference contrast and green fluorescence images. SVZ astrocyte progeny were traced with DAPI (blue). The resultant DAPI-stained colony grows on GFAP-positive cortical astrocytes (green) and yields a DAPI-positive cell colocalizing with the young neuronal marker TuJ1 (red), shown here at 10 d *in vitro*. Scale bars, 80 μm (**b**); 100 μm (**b** inset, **c**); 60 μm (**c** inset).

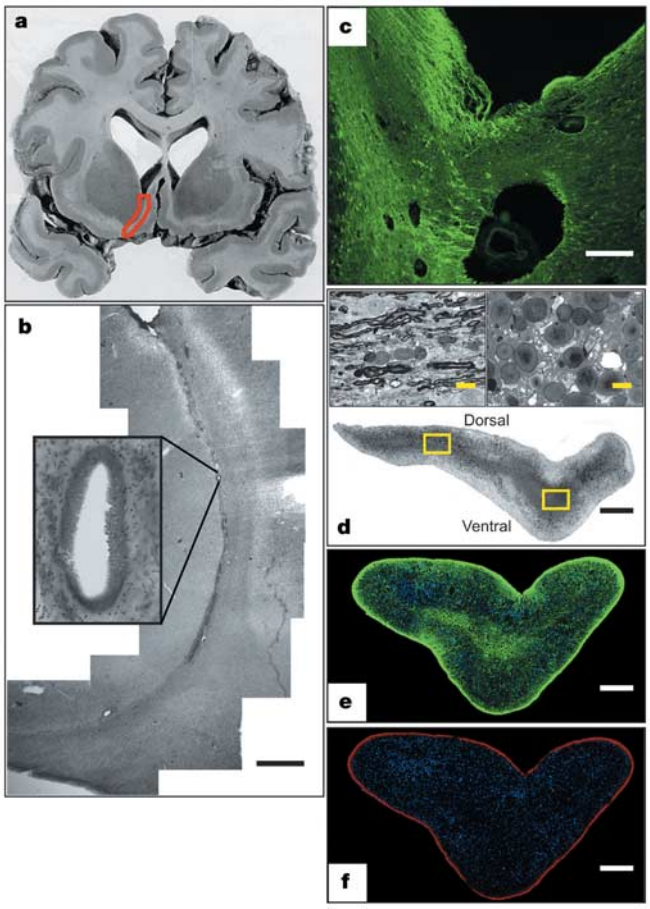

Figure 4 The human SVZ–olfactory trigone connection: no evidence for neuronal chain migration to the olfactory bulbs. **a**, Pathology specimen of the human brain region corresponding to the location of the mammalian RMS (red). **b**, Nissl staining of the human SVZ–olfactory trigone connection. Ependymal cavities (inset) suggest its embryonic ventricular origins. **c**, GFAP-positive fibres converge from the ventral floor of the anterior horn towards the olfactory trigone. **d**, Transverse section of the adult human olfactory peduncle. The left-hand box is magnified in the left inset, showing myelinated axons and oligodendrocytes; the right-hand box is magnified in the right inset, showing corpus amylaceum bodies found in the core of the olfactory peduncle. **e**, TuJ1 (red) and DAPI (blue) labelling of transverse olfactory peduncle, showing no evidence of chains of young neurons migrating to the olfactory bulb. **f**, GFAP (green) and DAPI (blue) labelling of transverse olfactory peduncle, showing abundant astrocytic processes, but no RMS. Scale bars, 5 mm (**b**); 500 μm (**c**, **d**); 25 μm (**d** insets); 400 μm (**e**, **f**).

Methods

Intraoperative and pathology specimens

Neurosurgical excisions of normal SVZ occurred as part of the planned margin of resection surrounding a periventricular lesion (Supplementary Table 1). We recorded the anatomical origin of each intraoperative specimen with stealth neuronavigation[29]. Intraoperative specimens were histologically normal with no evidence of dysplasia, and assessments were independently confirmed by a neuropathologist. For pathological specimens, autopsied brains were cut coronally at the temporal horn tip and immersed in 3% paraformaldehyde (PFA) or formalin for 1–2 weeks, and then portions of their lateral ventricular walls were excised (Supplementary Table 2). Autopsy specimens were obtained within 12 h of death from individuals who lacked clinical or postmortem evidence of brain pathology. All causes of death were non-neurological.

Expression of TuJ1 and PSA-NCAM was noted in different areas of brain parenchyma, indicating that the antibodies used recognized human antigen and that the human brain's antigenicity was preserved (Supplementary Fig. 3a, b). The *in vitro* and *in vivo* characteristics of human SVZ were observed in samples from individuals with different lesions and of different ages and sexes, and in intraoperative and pathology specimens alike, making it extremely unlikely that our results were due to specific diseases. Collection of all specimens was done in accordance with the University of California San Francisco Committee on Human Research.

Immunohistochemistry

All fixed specimens were rinsed in 0.1 M PBS and then cut on a vibratome (50 μm), cryostat (10 μm) or microtome (6 μm). Tissue sections were incubated overnight at 4 °C in blocking solution (PBS, 0.25% Triton X-100 and 10% normal donkey serum). Sections were then incubated for 48 h at 4 °C in primary antibody diluted in blocking solution. Primary antibodies dilutions were as follows: anti-GFAP (Chemicon), 1:500; anti-TuJ1 (Covance), 1:500; anti-Ki-67 (clone MIB-1, Dako), 1:50; anti-vimentin (Developmental Studies Hybridoma Bank), 1:1; anti-BrdU (Oxford Biotech), 1:10; and anti-PSA-NCAM (a gift from G. Rougon), 1:3,000. The antibody against O4 (Chemicon) was diluted to 1:100 in blocking solution without Triton X-100. After primary antibody incubation, sections were incubated for 18 h at 4 °C in secondary antibody (Jackson Laboratories) diluted 1:200. We used DAPI (1:5,000) for counterstaining, and Aqua Polymount (Polysciences) for mounting. In all experiments, omitting the primary antibody resulted in no labelling. Positive controls of rodent SVZ and human cortical specimens were analysed in parallel with experimental specimens.

Cell culture

Complete medium was a 0.2-μm filter-sterilized mixture of 44 ml of DMEM medium (Gibco), 5 ml of fetal calf serum, 0.5 ml of antibiotic or antimycotic and 0.5 ml of L-glutamine. After resection, intraoperative specimens were minced into 50–300-μm pieces, incubated in 0.25% trypsin and 0.02% versene for 10 min, triturated and plated onto uncoated T-25 flasks with complete medium. At confluence, flasks were shaken for 16 h at 300 r.p.m. to remove neurons, oligodendrocytes and microglia. This method[30] has been observed to yield cell cultures that are >98% GFAP positive[24].

Organotypic explant

Intraoperative human SVZ specimens were dissected in ice-cold complete medium under a microscope. Each 200-μm specimen was floated on a Millipore filter in a 35-mm dish with complete medium plus BrdU (10 ng μl^{-1}). After 36 h, specimens were immersed in 3% PFA for 24 h at 4 °C and then sectioned by cryostat. Immunohistochemistry was done as described above.

Neurosphere assay

Intraoperative specimens were dissociated as above and incubated in non-adherent neurosphere conditions as described[17]. Each 1-cm^2 well contained 1 ml of neurosphere medium[17] and a cell concentration of 50 cells per μl. Neurospheres were passaged at least three times without a significant difference in plating efficiency. Conditioned neurosphere medium was used only in clonal neurosphere assays, for which complete neurosphere medium was exposed to mature neurospheres for 24 h before the cells were filtered out. The resultant medium was combined in a 50:50 mixture with fresh complete neurosphere medium to generate conditioned neurosphere medium.

Cell division and astrocyte growth curve

The quantification of human astrocyte proliferation is described in the Supplementary Information.

Clonal monolayer assay

Single astrocytes, identified after 3 d of incubation with a GFAPp–GFP adenovirus[11], were incubated in DAPI (1:5,000) for 30 min at 37 °C and placed on a cortical astrocyte monolayer in 16-well glass slides with Neurobasal/B27 medium (Life Technologies). On the basis of immunohistochemistry, the specificity of the GFAPp–GFP adenovirus was >98% in human astrocyte cultures. Neurobasal/B27 medium was a mixture of 44 ml of DMEM-F12 medium, 5 ml of B27 supplement, 0.5 ml of L-glutamine and 0.5 ml of antibiotic or antimycotic. At 5–14 d *in vitro*, monolayers were fixed in PFA and processed with immunohistochemistry.

Electron microscopy

Specimens fixed in 2% glutaraldehyde and 2% paraformaldehyde were cut into 200-μm sections on a vibratome. Sections were post-fixed in 2% osmium, rinsed, dehydrated and embedded in Araldite (Durcupan, Fluka). To study SVZ architecture, we cut serial 1-μm semithin sections and stained them with 1% toluidine blue. To identify individual cell types, ultrathin (0.05-μm) sections were cut with a diamond knife, stained with lead citrate and examined under a Jeol 100CX electron microscope.

Received 24 June; accepted 19 December 2003; doi:10.1038/nature02301.

1. Alvarez-Buylla, A., Garcia-Verdugo, J. M. & Tramontin, A. D. A unified hypothesis on the lineage of neural stem cells. *Nature Rev. Neurosci.* **2,** 287–293 (2001).
2. Pincus, D. W. *et al. In vitro* neurogenesis by adult human epileptic temporal neocortex. *Clin. Neurosurg.* **44,** 17–25 (1997).
3. Roy, N. S. *et al.* Promoter-targeted selection and isolation of neural progenitor cells from the adult human ventricular zone. *J. Neurosci. Res.* **59,** 321–331 (2000).
4. Johansson, C. B., Svensson, M., Wallstedt, L., Janson, A. M. & Frisen, J. Neural stem cells in the adult human brain. *Exp. Cell Res.* **253,** 733–736 (1999).
5. Pagano, S. F. *et al.* Isolation and characterization of neural stem cells from the adult human olfactory bulb. *Stem Cells* **18,** 295–300 (2000).
6. Nunes, M. C. *et al.* Identification and isolation of multipotential neural progenitor cells from the subcortical white matter of the adult human brain. *Nature Med.* **9,** 439–447 (2003).
7. Kukekov, V. G. *et al.* Multipotent stem/progenitor cells with similar properties arise from two neurogenic regions of adult human brain. *Exp. Neurol.* **156,** 333–344 (1999).
8. Kornack, D. R. & Rakic, P. The generation, migration, and differentiation of olfactory neurons in the adult primate brain. *Proc. Natl Acad. Sci. USA* **98,** 4752–4757 (2001).
9. Alvarez-Buylla, A. & Garcia-Verdugo, J. M. Neurogenesis in adult subventricular zone. *J. Neurosci.* **22,** 629–634 (2002).
10. Pencea, V., Bingaman, K. D., Freedman, L. J. & Luskin, M. B. Neurogenesis in the subventricular zone and rostral migratory stream of the neonatal and adult primate forebrain. *Exp. Neurol.* **172,** 1–16 (2001).
11. Doetsch, F., Caille, I., Lim, D. A., Garcia-Verdugo, J. M. & Alvarez-Buylla, A. Subventricular zone astrocytes are neural stem cells in the adult mammalian brain. *Cell* **97,** 703–716 (1999).
12. Laywell, E. D., Rakic, P., Kukekov, V. G., Holland, E. C. & Steindler, D. A. Identification of a multipotent astrocytic stem cell in the immature and adult mouse brain. *Proc. Natl Acad. Sci. USA* **97,** 13883–13888 (2000).
13. Skogh, C. *et al.* Generation of regionally specified neurons in expanded glial cultures derived from the mouse and human lateral ganglionic eminence. *Mol. Cell. Neurosci.* **17,** 811–820 (2001).
14. Imura, T., Kornblum, H. I. & Sofroniew, M. V. The predominant neural stem cell isolated from postnatal and adult forebrain but not early embryonic forebrain expresses GFAP. *J. Neurosci.* **23,** 2824–2832 (2003).
15. Reynolds, B. A. & Weiss, S. Generation of neurons and astrocytes from isolated cells of the adult mammalian central nervous system. *Science* **255,** 1707–1710 (1992).
16. Chiasson, B. J., Tropepe, V., Morshead, C. M. & van der Kooy, D. Adult mammalian forebrain ependymal and subependymal cells demonstrate proliferative potential, but only subependymal cells have neural stem cell characteristics. *J. Neurosci.* **19,** 4462–4471 (1999).
17. Gritti, A. *et al.* Multipotent neural stem cells reside into the rostral extension and olfactory bulb of adult rodents. *J. Neurosci.* **22,** 437–445 (2002).
18. Kirschenbaum, B. *et al. In vitro* neuronal production and differentiation by precursor cells derived from the adult human forebrain. *Cereb. Cortex* **4,** 576–589 (1994).
19. Palmer, T. D. *et al.* Cell culture. Progenitor cells from human brain after death. *Nature* **411,** 42–43 (2001).
20. Doetsch, F., Garcia-Verdugo, J. M. & Alvarez-Buylla, A. Cellular composition and three-dimensional organization of the subventricular germinal zone in the adult mammalian brain. *J. Neurosci.* **17,** 5046–5061 (1997).
21. Blakemore, W. F. & Jolly, R. D. The subependymal plate and associated ependyma in the dog. An ultrastructural study. *J. Neurocytol.* **1,** 69–84 (1972).
22. Perez-Martin, M. *et al.* Ependymal explants from the lateral ventricle of the adult bovine brain: a model system for morphological and functional studies of the ependyma. *Cell Tissue Res.* **300,** 11–19 (2000).
23. Eriksson, P. S. *et al.* Neurogenesis in the adult human hippocampus. *Nature Med.* **4,** 1313–1317 (1998).
24. Lim, D. A. & Alvarez-Buylla, A. Interaction between astrocytes and adult subventricular zone precursors stimulates neurogenesis. *Proc. Natl Acad. Sci. USA* **96,** 7526–7531 (1999).
25. Song, H., Stevens, C. F. & Gage, F. H. Astroglia induce neurogenesis from adult neural stem cells. *Nature* **417,** 39–44 (2002).
26. Lois, C., Garcia-Verdugo, J. M. & Alvarez-Buylla, A. Chain migration of neuronal precursors. *Science* **271,** 978–981 (1996).
27. Bonfanti, L., Peretto, P., Merighi, A. & Fasolo, A. Newly-generated cells from the rostral migratory stream in the accessory olfactory bulb of the adult rat. *Neuroscience* **81,** 489–502 (1997).
28. Leel-Ossy, L. & Gati, I. Corpus amylaceum (polyglucosan body) in the peripheral olfactory system. *Pathol. Oncol. Res.* **4,** 212–216 (1998).
29. Smith, K. R., Frank, K. J. & Bucholz, R. D. The NeuroStation—a highly accurate, minimally invasive solution to frameless stereotactic neurosurgery. *Comput. Med. Imaging Graph.* **18,** 247–256 (1994).
30. McCarthy, K. D. & de Vellis, J. Preparation of separate astroglial and oligodendroglial cell cultures from rat cerebral tissue. *J. Cell Biol.* **85,** 890–902 (1980).

Supplementary Information accompanies the paper on **www.nature.com/nature**.

Acknowledgements We thank G. E. Vates and J. W. Chiong for comments on the manuscript; A. Bollen, D. Gaskin, T. Tihan and S. R. VandenBerg for assistance with pathology material; A. Leong for stealth neuronavigational imagery; and Z. Mirzadeh for imaging. This work was supported by a gift from Frances and John Bowes, by the William Siebrandt Glioblastoma Fund and grants from the NIH. A.A-B. is the Heather and Melanie Muss Professor. N.S. is supported by the HHMI and an American Brain Tumor Association David B. Anderson Fellowship. A.D.T. is supported by the Damon Runyon Cancer Research Foundation.

Competing interests statement The authors declare that they have no competing financial interests.

Correspondence and requests for materials should be addressed to N.S. (nsanai@itsa.ucsf.edu) or A.A.-B. (abuylla@itsa.ucsf.edu).